

Two-pion Bose–Einstein correlations in central Pb–Pb collisions
at $\sqrt{s_{NN}} = 2.76$ TeV

version 1.7
ALICE Collaboration

K. Aamodt^a, A. Abrahantes Quintana^b, D. Adamová^c, A.M. Adare^d, M.M. Aggarwal^e, G. Aglieri Rinella^f, A.G. Agocs^g, S. Aguilar Salazar^h, Z. Ahammedⁱ, N. Ahmadi^j, A. Ahmad Masoodi^j, S.U. Ahn^{k,1}, A. Akindinov^l, D. Aleksandrov^m, B. Alessandroⁿ, R. Alfaro Molina^h, A. Alici^{o,2}, A. Alkin^p, E. Almaráz Aviña^h, T. Alt^q, V. Altini^r, S. Altinpinar^s, I. Altsybeev^t, C. Andrei^u, A. Andronic^s, V. Anguelov^{v,3,1}, C. Anson^w, T. Antičić^x, F. Antinori^y, P. Antonioli^z, L. Aphecetche^{aa}, H. Appelshäuser^{ab}, N. Arbor^{ac}, S. Arcelli^o, A. Arend^{ab}, N. Armesto^{ad}, R. Arnaldiⁿ, T. Aronsson^d, I.C. Arsene^s, A. Asryan^t, A. Augustinus^f, R. Averbeck^s, T.C. Awes^{ae}, J. Äystö^{af}, M.D. Azmi^j, M. Bach^q, A. Badalà^{ag}, Y.W. Baek^{k,1}, S. Bagnascoⁿ, R. Bailhache^{ab}, R. Bala^{ah,5}, R. Baldini Ferroli^{ai}, A. Baldisseri^{aj}, A. Baldit^{ak}, J. Bán^{al}, R. Barbera^{am}, F. Barile^f, G.G. Barnaföldi^g, L.S. Barnby^{an}, V. Barret^{ak}, J. Bartke^{ao}, M. Basile^o, N. Bastid^{ak}, B. Bathen^{ap}, G. Batigne^{aa}, B. Batyunya^{aq}, C. Baumann^{ab}, I.G. Bearden^{ar}, H. Beck^{ab}, I. Belikov^{as}, F. Bellini^o, R. Bellwied^{at,6}, E. Belmont-Moreno^h, S. Beole^{ah}, I. Berceanu^u, A. Bercuci^u, E. Berdermann^s, Y. Berdnikov^{au}, L. Betev^f, A. Bhasin^{av}, A.K. Bhati^e, L. Bianchi^{ah}, N. Bianchi^{aw}, C. Bianchin^y, J. Bielčík^{ax}, J. Bielčíková^c, A. Bilandzic^{ay}, E. Biolcati^{ah}, A. Blanc^{ak}, F. Blanco^{az}, F. Blanco^{ba}, D. Blau^m, C. Blume^{ab}, M. Bocciofi^f, N. Bock^w, A. Bogdanov^{bb}, H. Bøggild^{ar}, M. Bogolyubsky^{bc}, L. Boldizsár^g, M. Bombara^{bd}, C. Bombinati^y, J. Book^{ab}, H. Borel^{aj}, C. Bortolin^{y,7}, S. Bose^{be}, F. Bossú^{ah}, M. Botje^{ay}, S. Böttger^v, B. Boyer^{bf}, P. Braun-Munzinger^s, L. Bravina^{bg}, M. Bregant^{bh,8}, T. Breitner^v, M. Broz^{bi}, R. Brun^f, E. Bruna^d, G.E. Bruno^r, D. Budnikov^{bj}, H. Buesching^{ab}, O. Busch^{bk}, Z. Buthelezi^{bl}, D. Caffarri^y, X. Cai^{bm}, H. Caines^d, E. Calvo Villar^{bn}, P. Camerini^{bh}, V. Canoa Roman^{f,9,1}, G. Cara Romeo^z, F. Carena^f, W. Carena^f, F. Carminati^f, A. Casanova Díaz^{aw}, M. Caselle^f, J. Castillo Castellanos^{aj}, V. Catanescu^u, C. Cavicchioli^f, P. Cerelloⁿ, B. Chang^{af}, S. Chapeland^f, J.L. Charvet^{aj}, S. Chattopadhyay^{be}, S. Chattopadhyayⁱ, M. Cherney^{bo}, C. Cheshkov^{bp}, B. Cheynis^{bp}, E. Chiavassaⁿ, V. Chibante Barroso^f, D.D. Chinellato^{bq}, P. Chochula^f, M. Chojnacki^{br}, P. Christakoglou^{br}, C.H. Christensen^{ar}, P. Christiansen^{bs}, T. Chujo^{bt}, C. Cicalo^{bu}, L. Cifarelli^o, F. Cindolo^z, J. Cleymans^{bl}, F. Coccetti^{ai}, J.-P. Coffin^{as}, S. Coliⁿ, G. Conesa Balbastre^{aw,11}, Z. Conesa del Valle^{aa,12}, P. Constantin^{bk}, G. Contin^{bh}, J.G. Contreras^{bv}, T.M. Cormier^{at}, Y. Corrales Morales^{ah}, I. Cortés Maldonado^{bw}, P. Cortese^{bx}, M.R. Cosentino^{bq}, F. Costa^f, M.E. Cotallo^{az}, E. Crescio^{bv}, P. Crochet^{ak}, E. Cuautle^{by}, L. Cunqueiro^{aw}, G. D Erasmo^r, A. Dainese^{bz,13}, H.H. Dalsgaard^{ar}, A. Danu^{ca}, D. Das^{be}, I. Das^{be}, A. Dash^{cb}, S. Dashⁿ, S. Deⁱ, A. De Azevedo Moregula^{aw}, G.O.V. de Barros^{cc}, A. De Caro^{cd}, G. de Cataldo^{ce}, J. de Cuveland^q, A. De Falco^{cf}, D. De Gruttola^{cd}, N. De Marcoⁿ, S. De Pasquale^{cd}, R. De Remigisⁿ, R. de Rooij^{br}, H. Delagrange^{aa}, Y. Delgado Mercado^{bn}, G. Dellacasa^{bx,14}, A. Deloff^{cg}, V. Demanov^{bj}, E. Dénes^g, A. Deppman^{cc}, D. Di Bari^f, C. Di Giglio^r, S. Di Liberto^{ch}, A. Di Mauro^f, P. Di Nezza^{aw}, T. Dietel^{ap}, R. Divià^f, Ø. Djuvsland^a, A. Dobrin^{at,15}, T. Dobrowolski^{cg}, I. Domínguez^{by}, B. Dönigus^s, O. Dordic^{bg}, O. Driga^{aa}, A.K. Dubeyⁱ, J. Dubuisson^f, L. Ducroux^{bp}, P. Dupieux^{ak}, A.K. Dutta Majumdar^{be}, M.R. Dutta Majumdarⁱ, D. Elia^{ce}, D. Emschermann^{ap}, H. Engel^v, H.A. Erdal^{ci}, B. Espagnon^{bf}, M. Estienne^{aa}, S. Esumi^{bt}, D. Evans^{an}, S. Evrard^f, G. Eyyubova^{bg}, C.W. Fabjan^{f,16}, D. Fabris^{cj}, J. Faivre^{ac}, D. Falchieri^o, A. Fantoni^{aw}, M. Fasel^s, R. Fearick^{bl}, A. Fedunov^{aq}, D. Fehlinger^a, V. Fekete^{bi}, D. Felea^{ca}, G. Feofilov^t, A. Fernández Téllez^{bw}, A. Ferretti^{ah}, R. Ferretti^{bx,17}, M.A.S. Figueredo^{cc}, S. Filchagin^{bj}, R. Fini^{ce}, D. Finogeev^{ck}, F.M. Fionda^r, E.M. Fiore^r, M. Floris^f, S. Foertsch^{bl}, P. Foka^{cs}, S. Fokin^m, E. Fragiadakis^{cm}, U. Frankfeld^s, U. Fuchs^f, F. Furano^f, C. Furget^{ac}, M. Fusco Girard^{cd}, J.J. Gaardhøje^{ar}, S. Gadrat^{ac}, M. Gagliardi^{ah}, A. Gago^{bn}, M. Gallio^{ah}, P. Ganoti^{cm,18}, C. Garabatos^{cs}, R. Gemme^{bx}, J. Gerhard^q, M. Germain^{aa}, C. Geuna^{aj}, A. Gheata^f, M. Gheata^f, B. Ghidini^f, P. Ghoshⁱ, M.R. Girard^{cn}, G. Giraudoⁿ, P. Giubellino^{ah,19}, E. Gladysz-Dziadus^{ao}, P. Glässel^{bk}, R. Gomez^{co}, L.H. González-Trueba^h, P. González-Zamora^{az}, H. González Santos^{bw}, S. Gorbunov^q, S. Gotovac^{cp}, V. Grabski^h, R. Grajcarek^{bk}, J. Gramling^{bk}, A. Grelli^{br}, A. Grigoras^f, C. Grigoras^f, V. Grigoriev^{bb}, A. Grigoryan^{cq}, S. Grigoryan^{aq}, B. Grinyov^p, N. Grion^{cl}, P. Gros^{bs}, J.F. Grosse-Oetringhaus^f, J.-Y. Grossiord^{bp}, R. Grosso^{cj}, F. Guber^{ck}, R. Guernane^{ac}, C. Guerra Gutierrez^{bn},

B. Guerzoni^o, K. Gulbrandsen^{ar}, T. Gunji^{cr}, A. Gupta^{av}, R. Gupta^{av}, H. Gutbrod^s, Ø. Haaland^d, C. Hadjidakis^{bf}, M. Haiduc^{ca}, H. Hamagaki^{cr}, G. Hamar^g, J.W. Harris^d, M. Hartig^{ab}, D. Hasch^{aw}, D. Hasegan^{ca}, D. Hatzifotiadou^z, A. Hayrapetyan^{ca,17}, M. Heide^{ap}, M. Heinz^d, H. Helstrup^{ci}, A. Herghelegiu^u, C. Hernández^s, G. Herrera Corral^{bv}, N. Herrmann^{bk}, K.F. Hetland^{ci}, B. Hicks^d, P.T. Hille^d, B. Hippolyte^{as}, T. Horaguchi^{bt}, Y. Hori^{cr}, P. Hristov^f, I. Hřivnáčová^{bf}, M. Huang^a, S. Huber^s, T.J. Humanic^w, D.S. Hwang^{cs}, R. Ichou^{aa}, R. Ilkaev^{bj}, I. Ilkiv^{cg}, M. Inaba^{bt}, E. Incani^{cf}, G.M. Innocenti^{ah}, P.G. Innocenti^f, M. Ippolitov^m, M. Irfan^j, C. Ivan^s, A. Ivanov^t, M. Ivanov^s, V. Ivanov^{au}, A. Jacholkowski^f, P.M. Jacobs^{ct}, L. Jancurová^{aq}, S. Jangal^{as}, R. Janik^{bi}, S.P. Jayarathna^{ba,20}, S. Jena^{cu}, L. Jirdeⁿ, G.T. Jones^{an}, P.G. Jones^{an}, P. Jovanović^{an}, H. Jung^k, W. Jung^k, A. Jusko^{an}, S. Kalcher^d, P. Kaliňák^{al}, M. Kalisky^{ap}, T. Kalliokoski^{af}, A. Kalweit^{cv}, R. Kamermans^{br,14}, K. Kanaki^a, E. Kang^k, J.H. Kang^{cw}, V. Kaplin^{bb}, O. Karavichev^{ck}, T. Karavicheva^{ck}, E. Karpechev^{ck}, A. Kazantsev^m, U. Keschull^v, R. Keidel^{cx}, M.M. Khan^j, A. Khanzadeev^{au}, Y. Kharlov^{bc}, B. Kileng^{ci}, D.J. Kim^{af}, D.S. Kim^k, D.W. Kim^k, H.N. Kim^k, J.H. Kim^{cs}, J.S. Kim^k, M. Kim^k, M. Kim^{cw}, S. Kim^{cs}, S.H. Kim^k, S. Kirsch^{f,21}, I. Kisel^{v,4}, S. Kiselev^l, A. Kisiel^f, J.L. Klay^{cy}, J. Klein^{bk}, C. Klein-Bösing^{ap}, M. Kliemant^{ab}, A. Klovning^a, A. Kluge^f, M.L. Knichel^s, K. Koch^{bk}, M.K. Köhler^s, R. Kolevatov^{bg}, A. Kolojvari^t, V. Kondratiev^t, N. Kondratyeva^{bb}, A. Konevskih^{ck}, E. Kornas^{ao}, C. Kottachchi Kankanamge Don^{at}, R. Kour^{an}, M. Kowalski^{ao}, S. Kox^{ac}, K. Kozlov^m, J. Kral^{af}, I. Králik^{al}, F. Kramer^{ab}, I. Kraus^{cv,22}, T. Krawutschke^{bk,23}, M. Kretz^q, M. Krivda^{an,24}, D. Krumbhorn^{bk}, M. Krus^{ax}, E. Kryshen^{au}, M. Krzewicki^{ay}, Y. Kucheriaev^m, C. Kuhn^{as}, P.G. Kuijjer^{ay}, P. Kurashvili^{cg}, A. Kurepin^{ck}, A.B. Kurepin^{ck}, A. Kuryakin^{bj}, S. Kushpil^c, V. Kushpil^c, M.J. Kweon^{bk}, Y. Kwon^{cw}, P. La Rocca^{am}, P. Ladrón de Guevara^{az,25}, V. Lafage^{bf}, C. Lara^v, D.T. Larsen^a, C. Lazzeroni^{an}, Y. Le Bornec^{bf}, R. Lea^{bh}, K.S. Lee^k, S.C. Lee^k, F. Lefèvre^{aa}, J. Lehnert^{ab}, L. Leistam^f, M. Lenhardt^{aa}, V. Lenti^{ce}, I. León Monzón^{co}, H. León Vargas^{ab}, P. Lévai^g, X. Li^{cz}, R. Lietava^{an}, S. Lindal^{bg}, V. Lindenstruth^{v,4}, C. Lippmann^{f,22}, M.A. Lisa^w, L. Liu^a, V.R. Loggins^{at}, V. Loginov^{bb}, S. Lohn^f, D. Lohner^{bk}, X. Lopez^{ak}, M. López Noriega^{bf}, E. López Torres^b, G. Løvhøiden^{bg}, X.-G. Lu^{bk}, P. Luettig^{ab}, M. Lunardon^y, G. Luparello^{ah}, L. Luquin^{aa}, C. Luzzi^f, K. Ma^{bm}, R. Ma^d, D.M. Madagodahettige-Don^{ba}, A. Maevskaya^{ck}, M. Mager^f, D.P. Mahapatra^{cb}, A. Maire^{as}, M. Malaev^{au}, I. Maldonado Cervantes^{by}, D. Mal'Kevich^l, P. Malzacher^s, A. Mamonov^{bj}, L. Manceau^{ak}, L. Mangotra^{av}, V. Manko^m, F. Manso^{ak}, V. Manzari^{ce}, Y. Mao^{bm,26}, J. Mareš^{da}, G.V. Margagliotti^{bh}, A. Margotti^z, A. Marín^s, I. Martashvili^{db}, P. Martinengo^f, M.I. Martínez^{bw}, A. Martínez Davalos^h, G. Martínez García^{aa}, Y. Martynov^p, A. Mas^{aa}, S. Masciocchi^s, M. Masera^{ah}, A. Masoni^{bu}, L. Massacrier^{bp}, M. Mastroarco^{ce}, A. Mastroserio^f, Z.L. Matthews^{an}, A. Matyjka^{ao,8}, D. Mayani^{by}, G. Mazzaⁿ, M.A. Mazzoni^{ch}, F. Meddi^{dc}, A. Menchaca-Rocha^h, P. Mendez Lorenzo^f, J. Mercado Pérez^{bk}, P. Mereuⁿ, Y. Miake^{bt}, J. Midori^{dd}, L. Milano^{ah}, J. Milosevic^{bg,27}, A. Mischke^{br}, D. Miśkowiec^{s,19}, C. Mitu^{ca}, J. Mlynarz^{at}, B. Mohantyⁱ, L. Molnar^f, L. Montaña Zetina^{bv}, M. Montenoⁿ, E. Montes^{az}, M. Morando^y, D.A. Moreira De Godoy^{cc}, S. Moretto^y, A. Morsch^f, V. Muccifora^{aw}, E. Mudnic^{cp}, H. Müller^f, S. Muhuriⁱ, M.G. Munhoz^{cc}, J. Muñoz^{bw}, L. Musaf^f, A. Mussoⁿ, B.K. Nandi^{cu}, R. Nania^z, E. Nappi^{ce}, C. Natrass^{db}, F. Navach^r, S. Navin^{an}, T.K. Nayakⁱ, S. Nazarenko^{bj}, G. Nazarov^{bj}, A. Nedosekin^l, F. Nendaz^{bp}, J. Newby^{de}, M. Nicassio^r, B.S. Nielsen^{ar}, S. Nikolaev^m, V. Nikolic^x, S. Nikulin^m, V. Nikulin^{au}, B.S. Nilsen^{bo}, M.S. Nilsson^{bg}, F. Noferini^z, G. Nooren^{br}, N. Novitzky^{af}, A. Nyani^m, A. Nyatha^{cu}, C. Nygaard^{ar}, J. Nystrand^a, H. Obayashi^{dd}, A. Ochirov^t, H. Oeschler^{cv}, S.K. Oh^k, J. Oleniacz^{cn}, C. Oppedisanoⁿ, A. Ortiz Velasquez^{by}, G. Ortona^{ah}, A. Oskarsson^{bs}, P. Ostrowski^{cn}, I. Otterlund^{bs}, J. Otwinowski^s, G. Øvrebek^a, K. Oyama^{bk}, K. Ozawa^{cr}, Y. Pachmayer^{bk}, M. Pachr^{ax}, F. Padilla^{ah}, P. Pagano^{cd}, G. Paic^{by}, F. Painke^q, C. Pajares^{ad}, S. Pal^{aj}, S.K. Palⁱ, A. Palaha^{an}, A. Palmeri^{ag}, G.S. Pappalardo^{ag}, W.J. Park^s, V. Patricchio^{ce}, A. Pavlinov^{at}, T. Pawlak^{cn}, T. Peitzmann^{br}, D. Peresunko^m, C.E. Pérez Lara^{ay}, D. Perini^f, D. Perrino^r, W. Peryt^{cn}, A. Pesci^z, V. Peskov^f, Y. Pestov^{df}, A.J. Peters^f, V. Petráček^{ax}, M. Petris^u, P. Petrov^{an}, M. Petrovici^u, C. Petta^{am}, S. Piano^{cl}, A. Piccottiⁿ, M. Pikna^{bi}, P. Pillot^{aa}, O. Pinazza^f, L. Pinsky^{ba}, N. Pitz^{ab}, F. Piuze^f, D.B. Piyarathna^{at,28}, R. Platt^{an}, M. Płoskoń^{ct}, J. Pluta^{cn}, T. Pocheptsov^{aq,29}, S. Pochybova^g, P.L.M. Podesta-Lerma^{co}, M.G. Poghosyan^{ah}, K. Polák^{da}, B. Polichtchouk^{bc}, A. Pop^u, V. Pospíšil^{ax}, B. Potukuchi^{av}, S.K. Prasad^{at,30}, R. Preghenella^{ai}, F. Prinoⁿ, C.A. Pruneau^{at}, I. Pshenichnov^{ck}, G. Puddu^{cf}, A. Pulvirenti^{am}, V. Punin^{bj}, M. Putiž^{bd}, J. Putschke^d, E. Quercigh^f, H. Qvigstad^{bg}, A. Rachevski^{cl}, A. Rademakers^f, O. Rademakers^f, S. Radomski^{bk}, T.S. Rähä^{af}, J. Rak^{af}, A. Rakotozafindrabe^{aj}, L. Ramello^{bx}, A. Ramírez Reyes^{bv}, M. Rammler^{ap}, R. Raniwala^{dg}, S. Raniwala^{dg}, S.S. Räsänen^{af}, K.F. Read^{db}, J.S. Real^{ac}, K. Redlich^{cg}, R. Renfordt^{ab}, A.R. Reolon^{aw}, A. Reshetin^{ck}, F. Rettig^q, J.-P. Revol^f, K. Reygiers^{bk}, H. Ricaud^{cv}, L. Riccatiⁿ, R.A. Ricci^{bz}, M. Richter^{a,31}, P. Riedler^f, W. Riegler^f, F. Riggi^{am}, A. Rivettiⁿ, M. Rodríguez Cahuantzi^{bw}, D. Rohr^d, D. Röhrich^a, R. Romita^s, F. Ronchetti^{aw}, P. Rosinsky^f, P. Rosnet^{ak}, S. Rossegger^f, A. Rossi^y, F. Roukoutakis^{cm}, S. Rousseau^{bf}, C. Roy^{aa,12}, P. Roy^{be}, A.J. Rubio Montero^{az}, R. Rui^{bh}, I. Rusanov^f, E. Ryabinkin^m, A. Rybicki^{ao}, S. Sadovsky^{bc}, K. Šafařík^f, R. Sahoo^y, P.K. Sahu^{cb}, P. Saiz^f, S. Sakai^{ct}

D. Sakata^{bt}, C.A. Salgado^{ad}, T. Samantaⁱ, S. Sambyal^{av}, V. Samsonov^{au}, L. Šándor^{al}, A. Sandoval^h, M. Sano^{bt}, S. Sano^{cf}, R. Santo^{ap}, R. Santoro^{ce}, J. Sarkamo^{af}, P. Saturnini^{ak}, E. Scapparone^z, F. Scarlassara^y, R.P. Scharenberg^{dh}, C. Schiaua^u, R. Schicker^{bk}, C. Schmidt^s, H.R. Schmidt^s, S. Schreiner^f, S. Schuchmann^{ab}, J. Schukraft^f, Y. Schutz^{aa,17}, K. Schwarz^s, K. Schweda^{bk}, G. Scioli^o, E. Scomparinⁿ, P.A. Scott^{an}, R. Scott^{db}, G. Segato^y, S. Senyukov^{bx}, J. Seo^k, S. Serci^{cf}, E. Serradilla^{az}, A. Sevcenco^{ca}, G. Shabratova^{aq}, R. Shahoyan^f, N. Sharma^e, S. Sharma^{av}, K. Shigaki^{dd}, M. Shimomura^{bt}, K. Shtejer^b, Y. Sibiriak^m, M. Siciliano^{ah}, E. Sicking^f, T. Siemiarzczuk^{cg}, A. Silenzi^o, D. Silvermyr^{ae}, G. Simonetti^{f,32}, R. Singarajuⁱ, R. Singh^{av}, B.C. Sinhaⁱ, T. Sinha^{be}, B. Sitar^{bi}, M. Sitta^{bx}, T.B. Skaali^{bg}, K. Skjerdal^a, R. Smakal^{ax}, N. Smirnov^d, R. Snellings^{ay,33}, C. Søggaard^{ar}, A. Soloviev^{bc}, R. Soltz^{de}, H. Son^{cs}, M. Song^{cw}, C. Soos^f, F. Soramel^y, M. Spyropoulou-Stassinaki^{cm}, B.K. Srivastava^{dh}, J. Stachel^{bk}, I. Stan^{ca}, G. Stefanek^{cg}, G. Stefanini^f, T. Steinbeck^{v,4}, E. Stenlund^{bs}, G. Steyn^{bl}, D. Stocco^{aa}, R. Stock^{ab}, M. Stolpovskiy^{bc}, P. Strmen^{bi}, A.A.P. Suaide^{cc}, M.A. Subieta Vázquez^{ah}, T. Sugitate^{dd}, C. Suire^{bf}, M. Šumbera^c, T. Susa^x, D. Swoboda^f, T.J.M. Symons^{ct}, A. Szanto de Toledo^{cc}, I. Szarka^{bi}, A. Szostak^a, C. Tagridis^{cm}, J. Takahashi^{bq}, J.D. Tapia Takaki^{bf}, A. Tauro^f, M. Tavlet^f, G. Tejada Muñoz^{bw}, A. Telesca^f, C. Terrevoli^r, J. Thäder^s, D. Thomas^{br}, J.H. Thomas^s, R. Tieulent^{bp}, A.R. Timmins^{at,6}, D. Tlusty^{ax}, A. Toia^f, H. Torii^{dd}, L. Toscano^f, F. Toselloⁿ, T. Traczyk^{cn}, D. Truesdale^w, W.H. Trzaska^{af}, A. Tumkin^{bj}, R. Turrisi^{cj}, A.J. Turvey^{bo}, T.S. Tveter^{bg}, J. Ulery^{ab}, K. Ullaland^a, A. Uras^{cf}, J. Urbán^{bd}, G.M. Urciuoli^{ch}, G.L. Usai^{cf}, A. Vacchi^{cl}, M. Vala^{aq,24}, L. Valencia Palomo^{bf}, S. Vallero^{bk}, N. van der Kolk^{ay}, M. van Leeuwen^{br}, P. Vande Vyvref, L. Vannucci^{bz}, A. Vargas^{bw}, R. Varma^{cu}, M. Vasileiou^{cm}, A. Vasiliev^m, V. Vechernin^t, M. Venaruzzo^{bh}, E. Vercellin^{ah}, S. Vergara^{bw}, R. Vernet^{di}, M. Verweij^{br}, L. Vickovic^{cp}, G. Viesti^y, O. Vikhlyantsev^{bj}, Z. Vilakazi^{bl}, O. Villalobos Baillie^{an}, A. Vinogradov^m, L. Vinogradov^t, Y. Vinogradov^{bj}, T. Virgili^{cd}, Y.P. Viyogiⁱ, A. Vodopyanov^{aq}, K. Voloshin^l, S. Voloshin^{at}, G. Volpe^r, B. von Haller^f, D. Vranic^s, J. Vrláková^{bd}, B. Vulpescu^{ak}, B. Wagner^a, V. Wagner^{ax}, R. Wan^{as,34}, D. Wang^{bm}, Y. Wang^{bk}, Y. Wang^{bm}, K. Watanabe^{bt}, J.P. Wessels^{ap}, U. Westerhoff^{ap}, J. Wiechula^{bk}, J. Wikne^{bg}, M. Wilde^{ap}, A. Wilk^{ap}, G. Wilk^{cg}, M.C.S. Williams^z, B. Windelband^{bk}, H. Yang^{aj}, S. Yasnopolskiy^m, J. Yi^{dj}, Z. Yin^{bm}, H. Yokoyama^{bt}, I.-K. Yoo^{dj}, X. Yuan^{bm}, I. Yushmanov^m, E. Zabrodin^{bg}, C. Zampolli^f, S. Zaporozhets^{aq}, A. Zarochentsev^t, P. Závada^{da}, H. Zbroszczyk^{cn}, P. Zelnicek^v, A. Zenin^{bc}, I. Zgura^{ca}, M. Zhalov^{au}, X. Zhang^{bm,1}, D. Zhou^{bm}, A. Zichichi^{o,35}, G. Zinoviev^p, Y. Zoccarato^{bp}, M. Zynovyev^p

^aDepartment of Physics and Technology, University of Bergen, Bergen, Norway

^bCentro de Aplicaciones Tecnológicas y Desarrollo Nuclear (CEADEN), Havana, Cuba

^cNuclear Physics Institute, Academy of Sciences of the Czech Republic, Řež u Prahy, Czech Republic

^dYale University, New Haven, Connecticut, United States

^ePhysics Department, Panjab University, Chandigarh, India

^fEuropean Organization for Nuclear Research (CERN), Geneva, Switzerland

^gKFKI Research Institute for Particle and Nuclear Physics, Hungarian Academy of Sciences, Budapest, Hungary

^hInstituto de Física, Universidad Nacional Autónoma de México, Mexico City, Mexico

ⁱVariable Energy Cyclotron Centre, Kolkata, India

^jDepartment of Physics Aligarh Muslim University, Aligarh, India

^kGangneung-Wonju National University, Gangneung, South Korea

^lInstitute for Theoretical and Experimental Physics, Moscow, Russia

^mRussian Research Centre Kurchatov Institute, Moscow, Russia

ⁿSezione INFN, Turin, Italy

^oDipartimento di Fisica dell'Università and Sezione INFN, Bologna, Italy

^pBogolyubov Institute for Theoretical Physics, Kiev, Ukraine

^qFrankfurt Institute for Advanced Studies, Johann Wolfgang Goethe-Universität Frankfurt, Frankfurt, Germany

^rDipartimento Interateneo di Fisica 'M. Merlin' and Sezione INFN, Bari, Italy

^sResearch Division and ExtreMe Matter Institute EMMI, GSI Helmholtzzentrum für Schwerionenforschung, Darmstadt, Germany

^tV. Fock Institute for Physics, St. Petersburg State University, St. Petersburg, Russia

^uNational Institute for Physics and Nuclear Engineering, Bucharest, Romania

^vKirchhoff-Institut für Physik, Ruprecht-Karls-Universität Heidelberg, Heidelberg, Germany

^wDepartment of Physics, Ohio State University, Columbus, Ohio, United States

^xRudjer Bošković Institute, Zagreb, Croatia

^yDipartimento di Fisica dell'Università and Sezione INFN, Padova, Italy

^zSezione INFN, Bologna, Italy

^{aa}SUBATECH, Ecole des Mines de Nantes, Université de Nantes, CNRS-IN2P3, Nantes, France

^{ab}Institut für Kernphysik, Johann Wolfgang Goethe-Universität Frankfurt, Frankfurt, Germany

^{ac}Laboratoire de Physique Subatomique et de Cosmologie (LPSC), Université Joseph Fourier, CNRS-IN2P3, Institut Polytechnique de Grenoble, Grenoble, France

^{ad}Departamento de Física de Partículas and IGFAE, Universidad de Santiago de Compostela, Santiago de Compostela, Spain

- ^{ae}Oak Ridge National Laboratory, Oak Ridge, Tennessee, United States
- ^{af}Helsinki Institute of Physics (HIP) and University of Jyväskylä, Jyväskylä, Finland
- ^{ag}Sezione INFN, Catania, Italy
- ^{ah}Dipartimento di Fisica Sperimentale dell'Università and Sezione INFN, Turin, Italy
- ^{ai}Centro Fermi – Centro Studi e Ricerche e Museo Storico della Fisica “Enrico Fermi”, Rome, Italy
- ^{aj}Commissariat à l’Energie Atomique, IRFU, Saclay, France
- ^{ak}Laboratoire de Physique Corpusculaire (LPC), Clermont Université, Université Blaise Pascal, CNRS-IN2P3, Clermont-Ferrand, France
- ^{al}Institute of Experimental Physics, Slovak Academy of Sciences, Košice, Slovakia
- ^{am}Dipartimento di Fisica e Astronomia dell'Università and Sezione INFN, Catania, Italy
- ^{an}School of Physics and Astronomy, University of Birmingham, Birmingham, United Kingdom
- ^{ao}The Henryk Niewodniczanski Institute of Nuclear Physics, Polish Academy of Sciences, Cracow, Poland
- ^{ap}Institut für Kernphysik, Westfälische Wilhelms-Universität Münster, Münster, Germany
- ^{aq}Joint Institute for Nuclear Research (JINR), Dubna, Russia
- ^{ar}Niels Bohr Institute, University of Copenhagen, Copenhagen, Denmark
- ^{as}Institut Pluridisciplinaire Hubert Curien (IPHC), Université de Strasbourg, CNRS-IN2P3, Strasbourg, France
- ^{at}Wayne State University, Detroit, Michigan, United States
- ^{au}Petersburg Nuclear Physics Institute, Gatchina, Russia
- ^{av}Physics Department, University of Jammu, Jammu, India
- ^{aw}Laboratori Nazionali di Frascati, INFN, Frascati, Italy
- ^{ax}Faculty of Nuclear Sciences and Physical Engineering, Czech Technical University in Prague, Prague, Czech Republic
- ^{ay}Nikhef, National Institute for Subatomic Physics, Amsterdam, Netherlands
- ^{az}Centro de Investigaciones Energéticas Medioambientales y Tecnológicas (CIEMAT), Madrid, Spain
- ^{ba}University of Houston, Houston, Texas, United States
- ^{bb}Moscow Engineering Physics Institute, Moscow, Russia
- ^{bc}Institute for High Energy Physics, Protvino, Russia
- ^{bd}Faculty of Science, P.J. Šafárik University, Košice, Slovakia
- ^{be}Saha Institute of Nuclear Physics, Kolkata, India
- ^{bf}Institut de Physique Nucléaire d’Orsay (IPNO), Université Paris-Sud, CNRS-IN2P3, Orsay, France
- ^{bg}Department of Physics, University of Oslo, Oslo, Norway
- ^{bh}Dipartimento di Fisica dell'Università and Sezione INFN, Trieste, Italy
- ^{bi}Faculty of Mathematics, Physics and Informatics, Comenius University, Bratislava, Slovakia
- ^{bj}Russian Federal Nuclear Center (VNIIEF), Sarov, Russia
- ^{bk}Physikalisches Institut, Ruprecht-Karls-Universität Heidelberg, Heidelberg, Germany
- ^{bl}Physics Department, University of Cape Town, iThemba Laboratories, Cape Town, South Africa
- ^{bm}Hua-Zhong Normal University, Wuhan, China
- ^{bn}Sección Física, Departamento de Ciencias, Pontificia Universidad Católica del Perú, Lima, Peru
- ^{bo}Physics Department, Creighton University, Omaha, Nebraska, United States
- ^{bp}Université de Lyon, Université Lyon 1, CNRS/IN2P3, IPN-Lyon, Villeurbanne, France
- ^{bq}Universidade Estadual de Campinas (UNICAMP), Campinas, Brazil
- ^{br}Nikhef, National Institute for Subatomic Physics and Institute for Subatomic Physics of Utrecht University, Utrecht, Netherlands
- ^{bs}Division of Experimental High Energy Physics, University of Lund, Lund, Sweden
- ^{bt}University of Tsukuba, Tsukuba, Japan
- ^{bu}Sezione INFN, Cagliari, Italy
- ^{bv}Centro de Investigación y de Estudios Avanzados (CINVESTAV), Mexico City and Mérida, Mexico
- ^{bw}Benemérita Universidad Autónoma de Puebla, Puebla, Mexico
- ^{bx}Dipartimento di Scienze e Tecnologie Avanzate dell'Università del Piemonte Orientale and Gruppo Collegato INFN, Alessandria, Italy
- ^{by}Instituto de Ciencias Nucleares, Universidad Nacional Autónoma de México, Mexico City, Mexico
- ^{bz}Laboratori Nazionali di Legnaro, INFN, Legnaro, Italy
- ^{ca}Institute of Space Sciences (ISS), Bucharest, Romania
- ^{cb}Institute of Physics, Bhubaneswar, India
- ^{cc}Universidade de São Paulo (USP), São Paulo, Brazil
- ^{cd}Dipartimento di Fisica ‘E.R. Caianiello’ dell'Università and Gruppo Collegato INFN, Salerno, Italy
- ^{ce}Sezione INFN, Bari, Italy
- ^{cf}Dipartimento di Fisica dell'Università and Sezione INFN, Cagliari, Italy
- ^{cg}Soltan Institute for Nuclear Studies, Warsaw, Poland
- ^{ch}Sezione INFN, Rome, Italy
- ^{ci}Faculty of Engineering, Bergen University College, Bergen, Norway
- ^{cj}Sezione INFN, Padova, Italy
- ^{ck}Institute for Nuclear Research, Academy of Sciences, Moscow, Russia
- ^{cl}Sezione INFN, Trieste, Italy
- ^{cm}Physics Department, University of Athens, Athens, Greece
- ^{cn}Warsaw University of Technology, Warsaw, Poland
- ^{co}Universidad Autónoma de Sinaloa, Culiacán, Mexico
- ^{cp}Technical University of Split FESB, Split, Croatia
- ^{cq}Yerevan Physics Institute, Yerevan, Armenia

- ^{ct}University of Tokyo, Tokyo, Japan
^{cs}Department of Physics, Sejong University, Seoul, South Korea
^{ct}Lawrence Berkeley National Laboratory, Berkeley, California, United States
^{cu}Indian Institute of Technology, Mumbai, India
^{cv}Institut für Kernphysik, Technische Universität Darmstadt, Darmstadt, Germany
^{cw}Yonsei University, Seoul, South Korea
^{cx}Zentrum für Technologietransfer und Telekommunikation (ZIT), Fachhochschule Worms, Worms, Germany
^{cy}California Polytechnic State University, San Luis Obispo, California, United States
^{cz}China Institute of Atomic Energy, Beijing, China
^{da}Institute of Physics, Academy of Sciences of the Czech Republic, Prague, Czech Republic
^{db}University of Tennessee, Knoxville, Tennessee, United States
^{dc}Dipartimento di Fisica dell'Università 'La Sapienza' and Sezione INFN, Rome, Italy
^{dd}Hiroshima University, Hiroshima, Japan
^{de}Lawrence Livermore National Laboratory, Livermore, California, United States
^{df}Budker Institute for Nuclear Physics, Novosibirsk, Russia
^{dg}Physics Department, University of Rajasthan, Jaipur, India
^{dh}Purdue University, West Lafayette, Indiana, United States
^{di}Centre de Calcul de l'IN2P3, Villeurbanne, France
^{dj}Pusan National University, Pusan, South Korea

Abstract

The first measurement of two-pion Bose–Einstein correlations in central Pb–Pb collisions at $\sqrt{s_{NN}} = 2.76$ TeV at the Large Hadron Collider is presented. The pion source radii and the decoupling time follow the trend established at lower energies and significantly exceed the ones measured at RHIC. The measurements are compared with model calculations.

Keywords: LHC, heavy-ion collisions, HBT, femtoscopy, intensity interferometry

1. Introduction

Matter at extremely high energy density created in central collisions of heavy ions at the Large Hadron Collider (LHC) is the main object of study of ALICE (A Large Ion Collider Experiment) [1, 2, 3]. The highly compressed strongly-interacting system created in these collisions is expected to undergo longitudinal and transverse expansion. The expansion rate and the final size at the time of hadron decoupling are accessible via intensity interferometry, a technique which exploits the Bose–Einstein enhancement of identical bosons emitted close in phase space. This approach, known as Hanbury Brown–Twiss analysis (HBT) [4, 5], has been successfully applied in e^+e^- [6], hadron–hadron and lepton–hadron [7], and heavy-ion [8] collisions.

2. Experiment and data analysis

In this Letter, we report on the first measurement of HBT radii in central Pb–Pb collisions at $\sqrt{s_{NN}} = 2.76$ TeV. The data were collected in November 2010, during the first lead beam running period of the LHC. During the runs used for this analysis the two beams had 4 or 66 bunches colliding at the ALICE interaction point. The bunch intensity was typically 7×10^7 Pb ions per bunch. The luminosity varied within $0.5 - 8 \times 10^{23} \text{ cm}^{-2} \text{ s}^{-1}$.

The detector readout was triggered by the LHC bunch crossing signal and a minimum-bias interaction trigger based on signals measured in the forward scintillators (VZERO) and in the Silicon Pixel Detector (SPD). The VZERO counters are placed along the beam line at +3.3 m and -0.9 m from the interaction point. They cover the region $2.8 < \eta < 5.1$ (VZERO-A) and $-3.7 < \eta < -1.7$ (VZERO-C) recording the amplitude and time of signals produced by charged particles. The

¹Also at Laboratoire de Physique Corpusculaire (LPC), Clermont Université, Université Blaise Pascal, CNRS-IN2P3, Clermont-Ferrand, France

²Now at Centro Fermi – Centro Studi e Ricerche e Museo Storico della Fisica “Enrico Fermi”, Rome, Italy

³Now at Physikalisches Institut, Ruprecht-Karls-Universität Heidelberg, Heidelberg, Germany

⁴Now at Frankfurt Institute for Advanced Studies, Johann Wolfgang Goethe-Universität Frankfurt, Frankfurt, Germany

⁵Now at Sezione INFN, Turin, Italy

⁶Now at University of Houston, Houston, Texas, United States

⁷Also at Dipartimento di Fisica dell’Università, Udine, Italy

⁸Now at SUBATECH, Ecole des Mines de Nantes, Université de Nantes, CNRS-IN2P3, Nantes, France

⁹Now at Centro de Investigación y de Estudios Avanzados (CINVESTAV), Mexico City and Mérida, Mexico

¹⁰Now at Benemérita Universidad Autónoma de Puebla, Puebla, Mexico

¹¹Now at Laboratoire de Physique Subatomique et de Cosmologie (LPSC), Université Joseph Fourier, CNRS-IN2P3, Institut Polytechnique de Grenoble, Grenoble, France

¹²Now at Institut Pluridisciplinaire Hubert Curien (IPHC), Université de Strasbourg, CNRS-IN2P3, Strasbourg, France

¹³Now at Sezione INFN, Padova, Italy

¹⁴Deceased

¹⁵Also at Division of Experimental High Energy Physics, University of Lund, Lund, Sweden

¹⁶Also at University of Technology and Austrian Academy of Sciences, Vienna, Austria

¹⁷Also at European Organization for Nuclear Research (CERN), Geneva, Switzerland

¹⁸Now at Oak Ridge National Laboratory, Oak Ridge, Tennessee, United States

¹⁹Now at European Organization for Nuclear Research (CERN), Geneva, Switzerland

²⁰Also at Wayne State University, Detroit, Michigan, United States

²¹Also at Frankfurt Institute for Advanced Studies, Johann Wolfgang Goethe-Universität Frankfurt, Frankfurt, Germany

²²Now at Research Division and ExtreMe Matter Institute EMMI, GSI Helmholtzzentrum für Schwerionenforschung, Darmstadt, Germany

²³Also at Fachhochschule Köln, Köln, Germany

²⁴Also at Institute of Experimental Physics, Slovak Academy of Sciences, Košice, Slovakia

²⁵Now at Instituto de Ciencias Nucleares, Universidad Nacional Autónoma de México, Mexico City, Mexico

²⁶Also at Laboratoire de Physique Subatomique et de Cosmologie (LPSC), Université Joseph Fourier, CNRS-IN2P3, Institut Polytechnique de Grenoble, Grenoble, France

²⁷Also at “Vinča” Institute of Nuclear Sciences, Belgrade, Serbia

²⁸Also at University of Houston, Houston, Texas, United States

²⁹Also at Department of Physics, University of Oslo, Oslo, Norway

³⁰Also at Variable Energy Cyclotron Centre, Kolkata, India

³¹Now at Department of Physics, University of Oslo, Oslo, Norway

³²Also at Dipartimento Interateneo di Fisica ‘M. Merlin’ and Sezione INFN, Bari, Italy

³³Now at Nikhef, National Institute for Subatomic Physics and Institute for Subatomic Physics of Utrecht University, Utrecht, Netherlands

³⁴Also at Hua-Zhong Normal University, Wuhan, China

³⁵Also at Centro Fermi – Centro Studi e Ricerche e Museo Storico della Fisica “Enrico Fermi”, Rome, Italy

two layers of SPD cover the central pseudorapidity regions $|\eta| < 2$ (inner) and $|\eta| < 1.4$ (outer). The detector has a total of 9.8 million pixels read out by 1200 chips. Each chip provides a fast signal if at least one of its pixels is hit. The signals from the 1200 chips are combined in a programmable logic unit which generates a trigger signal if hits are detected on at least two chips on the outer layer. The minimum-bias interaction trigger required at least two out of the following three conditions: i) two pixel chips hit in the outer layer of the SPD ii) a signal in VZERO-A iii) a signal in VZERO-C. More details of the trigger and run conditions are discussed in Ref. [9].

For the present analysis we have used 16 000 events selected by requiring a primary vertex reconstructed within ± 12 cm of the nominal interaction point and applying the centrality cut of 5% of the hadronic cross section. The centrality was derived from the total amplitude measured in the VZERO detector. The charged-particle pseudorapidity density measured in this centrality class is $\langle dN_{\text{ch}}/d\eta \rangle = 1584 \pm 4$ (stat) ± 76 (syst) as published in Ref. [9] where the centrality determination and the measurement of charged-particle pseudorapidity density are described in detail.

The correlation analysis was performed using charged-particle tracks detected in the Time Projection Chamber (TPC). The TPC is a cylindrical drift detector with two readout planes on the endcaps. The active volume covers $85 < r < 247$ cm and $-250 < z < 250$ cm in the radial and longitudinal directions, respectively. A high voltage membrane at $z = 0$ divides the active volume into two halves and provides the electric drift field of 400 V/cm, resulting in a maximum drift time of 94 μs . With the solenoidal magnetic field of 0.5 T the momentum resolution for particles with $p_T < 1$ GeV/c is better than 1%. Tracks at the edge of the acceptance were suppressed by restricting the analysis to the region $|\eta| < 0.8$. Good track quality was ensured by requiring the tracks to have at least 90 clusters in the TPC (out of a maximum of 159), to have at least two matching hits in the Inner Tracking System (ITS) (out of a maximum of 6), and to point back to the primary interaction vertex within 1 cm. Although not critical for this analysis (see discussion of the systematic uncertainties below) pions were identified via their specific ionization (dE/dx) in the TPC gas. In central Pb–Pb collisions the dE/dx resolution of the TPC is better than 7%.

3. Two-pion correlation functions

The two-particle correlation function is defined as the ratio $C(\mathbf{q}) = A(\mathbf{q})/B(\mathbf{q})$, where $A(\mathbf{q})$ is the mea-

sured distribution of pair momentum difference $\mathbf{q} = \mathbf{p}_2 - \mathbf{p}_1$, with the three-momenta of the two particles \mathbf{p}_1 and \mathbf{p}_2 , and $B(\mathbf{q})$ is a similar distribution formed by using pairs of particles from different events (event mixing) [10]. The momentum difference was calculated in the longitudinally co-moving system (LCMS), where the longitudinal pair momentum vanishes, and is decomposed into $(q_{\text{out}}, q_{\text{side}}, q_{\text{long}})$, with the “out” axis pointing along the pair transverse momentum, the “side” axis perpendicular to it in the transverse plane, and the “long” axis along the beam (Bertsch–Pratt convention [11, 12]). The correlation functions were studied in bins of transverse momentum, defined as half the module of the vector sum of the two transverse momenta, $k_T = |\mathbf{p}_{T,1} + \mathbf{p}_{T,2}|/2$. During event mixing, every event was mixed with five other events, and all pion tracks from one event were paired with all pion tracks from the other event.

Track splitting (incorrect reconstruction of a track left by one particle as two tracks) and track merging (reconstructing one track instead of two) in the event reconstruction generally lead to structures in the two-particle correlation functions if not properly treated. The track splitting effect is negligible in our data. The track merging, with the particular track selection used in this analysis, reduces the two-track reconstruction efficiency to 70–80% for track pairs with a distance of closest approach in the TPC of 1 cm or less. We have removed this effect by suppressing, in the numerator and the denominator of the correlation function, all track pairs separated by less than 1.2 cm transversally and 2.4 cm longitudinally at a radius of 1.2 m. We have checked that by applying this cut one recovers the flat shape of the correlation function in Monte Carlo simulation.

Projections of three-dimensional two-pion correlation functions $C(q_{\text{out}}, q_{\text{side}}, q_{\text{long}})$ for seven k_T bins are shown in Fig. 1. The Bose–Einstein enhancement peak is manifest at low $q = |\mathbf{q}|$. The peak width increases when going from low to high transverse momenta. The three-dimensional correlation functions were fitted by a function accounting for the Bose–Einstein enhancement and for the Coulomb interaction between the two particles:

$$\begin{aligned} C(\mathbf{q}) &= (1 - \lambda) + \lambda K(q_{\text{inv}})(1 + G(\mathbf{q})), \\ G(\mathbf{q}) &= \exp(-(R_{\text{out}}^2 q_{\text{out}}^2 + R_{\text{side}}^2 q_{\text{side}}^2 + R_{\text{long}}^2 q_{\text{long}}^2 + |R_{\text{ol}}| R_{\text{ol}} q_{\text{out}} q_{\text{long}})), \end{aligned} \quad (1)$$

with λ describing the correlation strength, and R_{out} , R_{side} , and R_{long} being the Gaussian HBT radii [13]. The

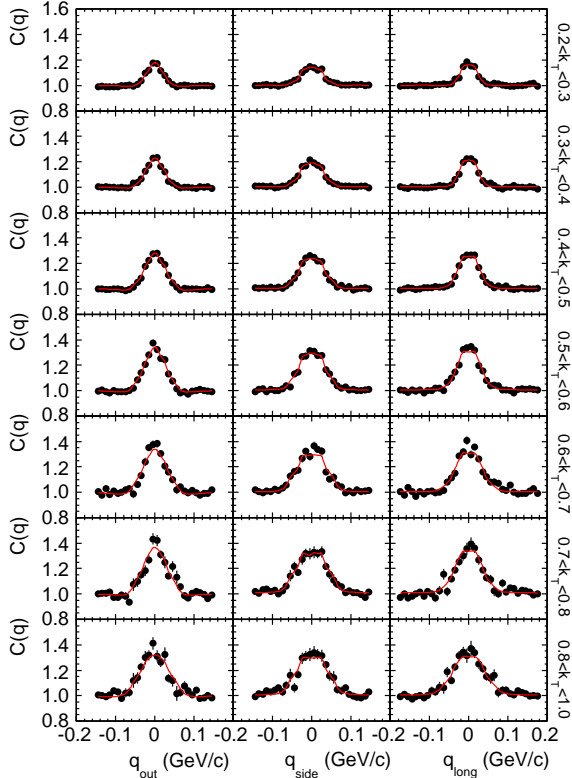


Figure 1: Projections of the three-dimensional $\pi^-\pi^-$ correlation function (points) and of the respective fits (line) for seven k_T bins. When projecting on one axis the other two components were required to be within $(-0.3, 0.3)$ GeV/c. The transverse momentum k_T is indicated on the right hand side axis in GeV/c.

parameter R_{0l} , that quantifies the cross term between q_{out} and q_{long} , turned out to be consistent with zero, as expected for measurements at midrapidity in a symmetric system. This term was therefore set equal to zero in the final fits. The factor K is the squared Coulomb wave function averaged over a spherical source of size equal to the mean of R_{out} , R_{side} , and R_{long} . It is attenuated by the same factor λ as the Bose–Einstein peak. The fit function is shown as the solid line in Fig. 1.

The obtained radii have to be corrected for the finite momentum resolution that smears out the correlation peak. The effect was studied by applying weights to pairs of tracks in simulated events so as to produce the correlation function expected for a given value of the HBT radius. The weights are calculated using the original Monte Carlo momenta. The reconstructed radii were found to differ from the input ones by up to 4%, depending on the radius and k_T . The corresponding correction was applied to the experimental HBT radii and λ .

4. Systematic uncertainties

The systematic uncertainties on the HBT parameters were estimated by comparing the results obtained when varying the analysis procedure. Not requiring the ITS hits in the tracking leads to a variation of the transverse and longitudinal radii by up to 3% and 8%, respectively. The effect of contamination of the pion sample by electrons and kaons was tested by loosening the PID selection pion identification criteria. This was found to introduce radius variations by up to 5%. Changing the fit range in q from 0-0.3 GeV/c to 0-0.5 GeV/c results in a reduction of all three radii by about 3%. Variation of the two-track separation condition by 50% results in a change of the radii by up to 3%. Generating the denominator of the correlation function by rotating one of the two tracks by 180° rather than by event mixing results in a 6% increase of R_{side} at low k_T and up to 4% for R_{out} and R_{long} . The systematic error connected to the Coulomb correction was evaluated by modifying the source radius used for the correction by ± 2 fm. This was found to affect mostly R_{out} which changes by up to 4%. The correction for the momentum resolution is about 4%; the corresponding uncertainty on final radii, tested by modifying the momentum resolution by 20% and by using different parametrizations, is negligible. Finally, a completely independent analysis, including a different pair selection criterion, yields transverse radii and R_{long} that differ by up to 5% and 8%, respectively. The total systematic errors were calculated by adding up the mentioned contributions in quadrature and reach up to 10%.

5. Transverse momentum dependence of the radii

The HBT radii extracted from the fit to the two-pion correlation functions and corrected for the momentum resolution as described in the previous section are shown as a function of k_T in Table 1 and in Fig. 2. The fit parameters for positive and negative pion pairs agree within statistical errors and therefore the averages are presented here. The HBT radii for the most central 5% Pb–Pb collisions at $\sqrt{s_{NN}} = 2.76$ TeV are found to be 10-35% larger than those measured in central Au–Au collisions at $\sqrt{s_{NN}} = 200$ GeV [14]. As also observed in heavy-ion collision experiments at lower energies [8], the HBT radii show a decreasing trend with increasing k_T . This is a characteristic feature of expanding particle sources since the HBT radii describe the homogeneity length rather than the overall size of the particle-emitting system [15, 16]. The homogeneity length is defined as the size of the region that contributes to the

Table 1: Extracted pion HBT parameters as function of k_T .

$\langle k_T \rangle$ (GeV/c)	λ	R_{out} (fm)	R_{side} (fm)	R_{long} (fm)
0.26	0.49 ± 0.01 (stat)	6.92 ± 0.12 (stat) ± 0.61 (syst)	6.36 ± 0.12 (stat) ± 0.54 (syst)	8.03 ± 0.15 (stat) ± 0.41 (syst)
0.35	0.57 ± 0.01 (stat)	6.03 ± 0.08 (stat) ± 0.48 (syst)	6.13 ± 0.09 (stat) ± 0.26 (syst)	7.31 ± 0.10 (stat) ± 0.39 (syst)
0.44	0.58 ± 0.01 (stat)	5.15 ± 0.07 (stat) ± 0.30 (syst)	5.49 ± 0.08 (stat) ± 0.30 (syst)	6.23 ± 0.09 (stat) ± 0.41 (syst)
0.54	0.65 ± 0.02 (stat)	4.79 ± 0.08 (stat) ± 0.34 (syst)	5.14 ± 0.09 (stat) ± 0.26 (syst)	5.67 ± 0.10 (stat) ± 0.35 (syst)
0.64	0.67 ± 0.02 (stat)	4.56 ± 0.10 (stat) ± 0.29 (syst)	4.73 ± 0.11 (stat) ± 0.25 (syst)	5.30 ± 0.12 (stat) ± 0.40 (syst)
0.75	0.65 ± 0.03 (stat)	4.29 ± 0.12 (stat) ± 0.34 (syst)	4.48 ± 0.13 (stat) ± 0.20 (syst)	4.90 ± 0.15 (stat) ± 0.50 (syst)
0.88	0.59 ± 0.03 (stat)	4.02 ± 0.14 (stat) ± 0.26 (syst)	4.35 ± 0.14 (stat) ± 0.34 (syst)	4.43 ± 0.15 (stat) ± 0.44 (syst)

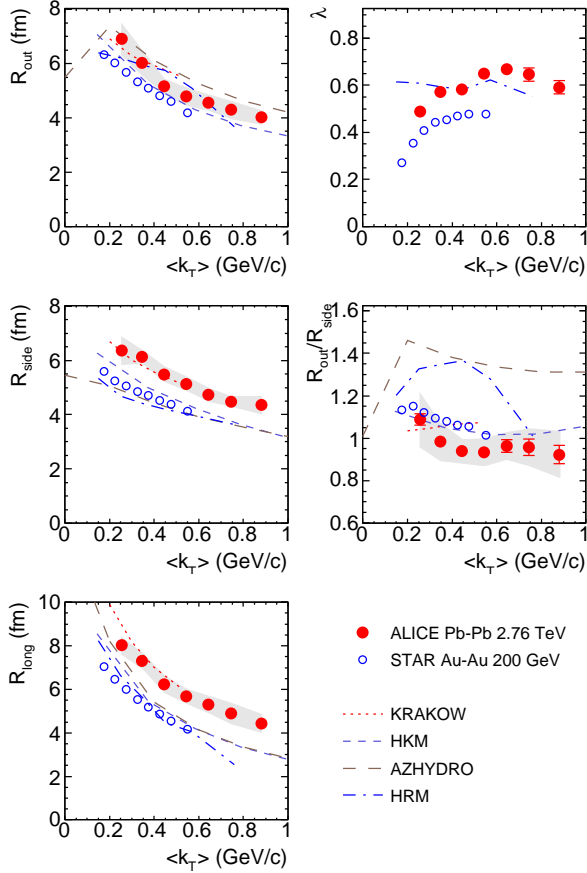


Figure 2: Pion HBT parameters for the most central 5% fraction of Pb–Pb collisions at $\sqrt{s_{\text{NN}}} = 2.76$ TeV, as function of k_T (red filled dots). The shaded bands represent the systematic errors. For comparison, parameters for Au–Au collisions at $\sqrt{s_{\text{NN}}} = 200$ GeV [14] are shown as blue open circles. The lines show model predictions (see text for discussion).

pion spectrum at a particular \mathbf{p} value. The R_{out} radius is comparable with R_{side} and the k_T dependence of the ratio $R_{\text{out}}/R_{\text{side}}$ is flat within the systematic errors. R_{long} is seen to be somewhat larger than R_{out} and R_{side} and to decrease slightly faster with increasing k_T .

The extracted λ -parameter is found to range from

0.49 to 0.67 and increases slightly with increasing k_T . Somewhat lower values but a similar k_T dependence was observed in Au–Au collisions at RHIC [14].

Also shown in Fig. 2 are the predictions of three models incorporating hydrodynamic approach, AZHYDRO [17], KRAKOW [18, 19], and HKM [20, 21], and of the hadronic-kinematics-based model HRM [22, 23]. KRAKOW [18] and HRM [23] provide predictions for the energy of $\sqrt{s_{\text{NN}}} = 2.76$ TeV; their calculations of $dN_{\text{ch}}/d\eta$ are off by +36% and -24%, respectively. The HKM [20] calculation was performed for a charged-particle pseudorapidity density of $dN_{\text{ch}}/d\eta = 1500$ close to the actual $\langle dN_{\text{ch}}/d\eta \rangle$ of the event sample used in the present analysis. Out of the five sets of radii provided by AZHYDRO [17] the one with an initial entropy density of 458 fm^{-3} gives the closest charged-particle pseudorapidity density ($dN_{\text{ch}}/d\eta = 1450$) and thus is used for the comparison.

All four models predict the decreasing trend of the radii with increasing k_T . AZHYDRO underpredicts R_{side} but comes close to the data for R_{out} and R_{long} . KRAKOW and HKM predict values close to the experimental ones for all three radii. In particular, they predict R_{out} to increase less than R_{side} between RHIC and LHC central collisions, resulting in an $R_{\text{out}}/R_{\text{side}}$ ratio close to unity. In both models this is a consequence of the transformation from “inside-out” to “outside-in” freeze-out (or from negative to positive $r - t$ correlation at freeze-out). The hadronic model HRM underpredicts the value of R_{side} and comes closer for R_{out} and R_{long} .

The predictions of the λ -parameter by HRM are also shown in Fig. 2. As seen, HRM comes close to the experimental values. In this model the value of λ is mostly determined by the presence of long-lived resonances which decay into pions, e.g. η and η' .

6. Energy dependence

In the left panel of Fig. 3, we compare the three radii at $\langle k_T \rangle = 0.3$ GeV/c with experimental results at lower energies. The value of the radius at this k_T was obtained

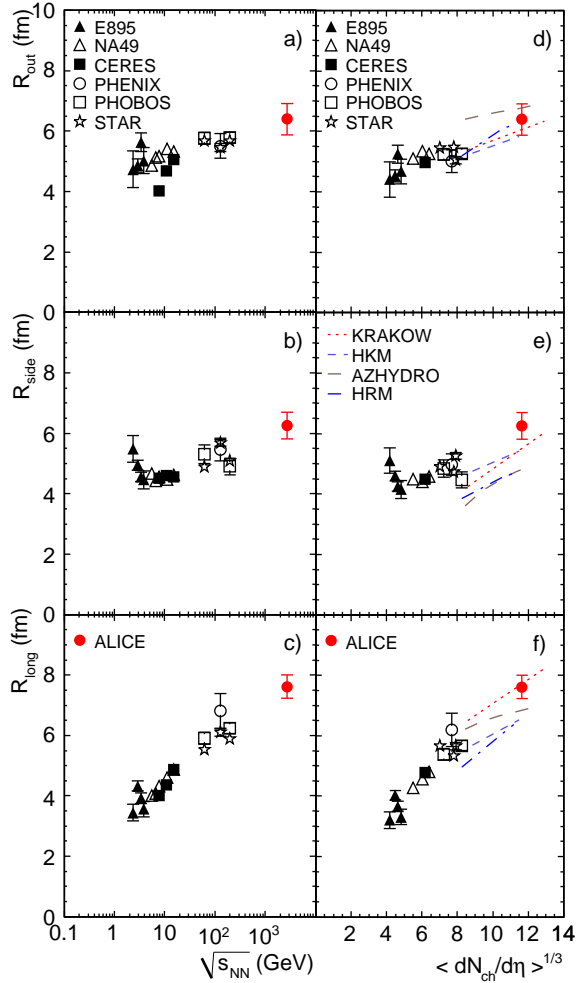


Figure 3: Pion HBT radii at $k_T = 0.3$ GeV/c for top central 5% Pb–Pb at $\sqrt{s_{NN}} = 2.76$ TeV (red filled dot) and the radii obtained for central gold and lead collisions at the AGS [24], SPS [25, 26, 27], and RHIC [14, 28, 29, 30, 31, 32, 33, 34], plotted versus the energy (panels a-c) and versus the cube root of charged-particle pseudorapidity density (panels d-f). Model predictions are shown as lines. For the ALICE point the error bar is dominated by the systematic uncertainties.

by parabolic interpolation of the measured or calculated radii. The radii were scaled to the Pb–Pb system (factor $(208^2/AB)^{1/3}$), with A and B denoting the mass numbers of the colliding ions, and to the top 5% centrality (factor $(N_{part}^{5\%}/\langle N_{part}^{meas} \rangle)^{1/3}$). All three radii smoothly increase with energy, although the transverse radii change slower than R_{long} . The ALICE measurement significantly broadens the range of the existing world systematics of HBT radii.

Since for hydrodynamical models the particle multiplicity is a better variable than the collision energy, in

order to compare our results to the models we plot, in the right panel of Fig. 3, the radii versus the cube root of charged-particle pseudorapidity density. For fixed target experiments and for those that quote the multiplicity in terms of $dN_{ch}/d\eta$ we apply a conversion factor of 0.88 so one can compare them to $dN_{ch}/d\eta$ from collider experiments. The radii are found to increase roughly linearly with $\langle dN_{ch}/d\eta \rangle^{1/3}$. The increase is in fair agreement with the predictions of the four models.

The collision energy dependence of the product of the three radii is shown in the top panel of Fig. 4. The product of the radii, which is connected with the volume of the homogeneity region, is nearly two times larger at the LHC than at RHIC. Because of expansion, the homogeneity region represents only a fraction of the total particle-emitting system.

The total longitudinal size of the system at the time when the midrapidity hadrons freeze-out can be estimated as explained in the following. The size of the homogeneity region is inversely proportional to the velocity gradient of the expanding system. The longitudinal velocity gradient in a high energy nuclear collision decreases with time as $1/\tau$. Therefore, the magnitude of R_{long} is proportional to the total duration of the longitudinal expansion, i.e. to the decoupling time τ_f of the system [35]. The decoupling time τ_f can be obtained by fitting R_{long} with

$$R_{long}^2(k_T) = \frac{\tau_f^2 T}{m_T} \frac{K_2(m_T/T)}{K_1(m_T/T)}, \quad m_T = \sqrt{m_\pi^2 + k_T^2}, \quad (2)$$

where m_π is the pion mass, T the kinetic freeze-out temperature taken to be 0.12 GeV, and K_1 and K_2 are the integer order modified Bessel functions [35, 36]. The lower panel of Fig. 4 shows the extracted expansion time τ_f together with results of the same fit to the published HBT radii at lower energies. As can be seen, τ_f follows a linear dependence with $\log(\sqrt{s_{NN}})$ and reaches 10–11 fm/c at 2.76 GeV. Finally, since the two ends of the expanding system recede with the velocity of light, the total length at the time when the midrapidity hadrons decouple can be estimated as $2\tau_f c$.

While Eq. (2) captures basic features of a longitudinally expanding particle-emitting system it should be noted that in the presence of transverse expansion and a finite chemical potential of pions it may underestimate the actual decoupling time by about 25% [37]. Another uncertainty is connected to the value of the kinetic freeze-out temperature used in the fit. While the value 0.12 GeV used is reasonably consistent with the temperature extracted from a simultaneous description

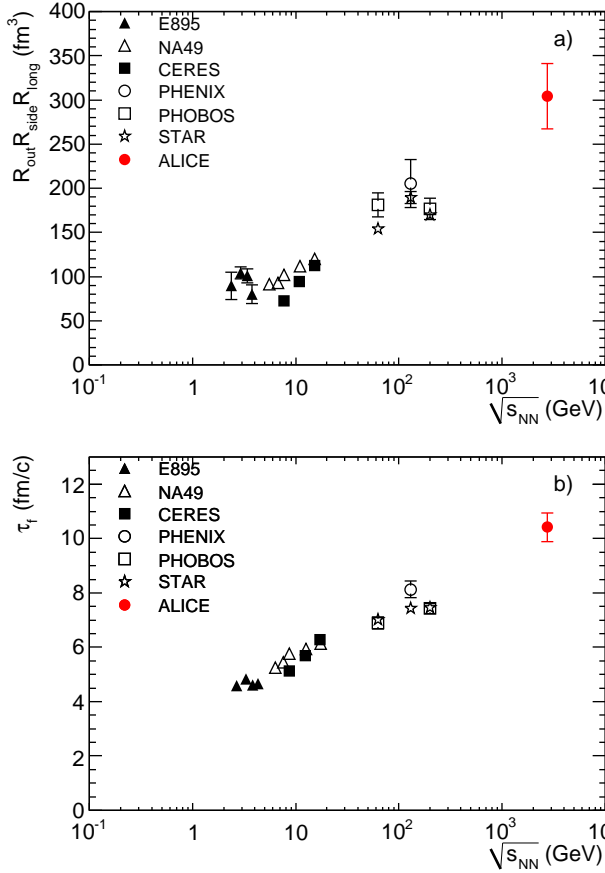


Figure 4: Product of the three pion HBT radii at $k_T = 0.3$ GeV/c (top) and the decoupling time extracted from $R_{\text{long}}(k_T)$ (bottom). The ALICE results (red filled dots) are compared to those obtained for central gold and lead collisions at lower energies at the AGS [24], SPS [25, 26, 27], and RHIC [14, 28, 29, 30, 31, 32, 33, 34].

of transverse momentum spectra of different particle species at RHIC and SPS, analyses including experimental HBT radii typically lead to temperatures around 0.1 GeV or below [38, 25, 14]. Assuming $T=0.10$ GeV leads to a 12% higher value for τ_f .

7. Summary

In summary, we have presented the first analysis of the two-pion correlation functions in Pb–Pb collisions at $\sqrt{s_{\text{NN}}} = 2.76$ TeV at the LHC. The pion source radii deduced from this measurement exceed the ones measured at RHIC by 10-35%. This behaviour is in fair agreement with model predictions. The decoupling time, that can be identified with the total duration of the reaction, exceeds 10 fm/c which is 30% larger than at RHIC.

Acknowledgements

The ALICE collaboration would like to thank all its engineers and technicians for their invaluable contributions to the construction of the experiment and the CERN accelerator teams for the outstanding performance of the LHC complex. The ALICE collaboration acknowledges the following funding agencies for their support in building and running the ALICE detector: Calouste Gulbenkian Foundation from Lisbon and Swiss Fonds Kidagan, Armenia; Conselho Nacional de Desenvolvimento Científico e Tecnológico (CNPq), Financiadora de Estudos e Projetos (FINEP), Fundação de Amparo à Pesquisa do Estado de São Paulo (FAPESP); National Natural Science Foundation of China (NSFC), the Chinese Ministry of Education (CMOE) and the Ministry of Science and Technology of China (MSTC); Ministry of Education and Youth of the Czech Republic; Danish Natural Science Research Council, the Carlsberg Foundation and the Danish National Research Foundation; The European Research Council under the European Community's Seventh Framework Programme; Helsinki Institute of Physics and the Academy of Finland; French CNRS-IN2P3, the 'Region Pays de Loire', 'Region Alsace', 'Region Auvergne' and CEA, France; German BMBF and the Helmholtz Association; Greek Ministry of Research and Technology; Hungarian OTKA and National Office for Research and Technology (NKTH); Department of Atomic Energy and Department of Science and Technology of the Government of India; Istituto Nazionale di Fisica Nucleare (INFN) of Italy; MEXT Grant-in-Aid for Specially Promoted Research, Japan; Joint Institute for Nuclear Research, Dubna; National Research Foundation of Korea (NRF); CONACYT, DGAPA, México, ALFA-EC and the HELLEN Program (High-Energy physics Latin-American–European Network); Stichting voor Fundamenteel Onderzoek der Materie (FOM) and the Nederlandse Organisatie voor Wetenschappelijk Onderzoek (NWO), Netherlands; Research Council of Norway (NFR); Polish Ministry of Science and Higher Education; National Authority for Scientific Research - NASR (Autoritatea Națională pentru Cercetare Științifică - ANCS); Federal Agency of Science of the Ministry of Education and Science of Russian Federation, International Science and Technology Center, Russian Academy of Sciences, Russian Federal Agency of Atomic Energy, Russian Federal Agency for Science and Innovations and CERN-INTAS; Ministry of Education of Slovakia; CIEMAT, EELA, Ministerio de Educación y Ciencia of Spain, Xunta de Galicia (Consellería de Educación), CEADEN, Cubaenergía, Cuba, and IAEA (Intern-

375 tional Atomic Energy Agency); The Ministry of Science and Technology and the National Research Foundation (NRF), South Africa; Swedish Research Council (VR) and Knut & Alice Wallenberg Foundation (KAW); Ukraine Ministry of Education and Science; United Kingdom Science and Technology Facilities Council (STFC); The United States Department of Energy, the United States National Science Foundation, the State of Texas, and the State of Ohio.

384 References

385 [1] K. Aamodt, et al., The ALICE experiment at the CERN LHC, JINST 3 (2008) S08002. doi:10.1088/1748-0221/3/08/S08002.

386 [2] F. Carminati, (ed.), et al., ALICE: Physics performance report, volume I, J. Phys. G30 (2004) 1517–1763. doi:10.1088/0954-3899/30/11/001.

387 [3] B. Alessandro, (Ed.), et al., ALICE: Physics performance report, volume II, J. Phys. G32 (2006) 1295–2040. doi:10.1088/0954-3899/32/10/001.

388 [4] R. Hanbury Brown, R. Twiss, Nature 178 (1956) 1046.

389 [5] R. Hanbury Brown, R. Q. Twiss, A New type of interferometer for use in radio astronomy, Phil. Mag. 45 (1954) 663–682.

390 [6] W. Kittel, Bose-Einstein correlations in Z fragmentation and other reactions, Acta Phys. Polon. B32 (2001) 3927–3972. arXiv:hep-ph/01110088.

391 [7] G. Alexander, Bose-einstein and fermi-dirac interferometry in particle physics, Rept. Prog. Phys. 66 (2003) 481–522. arXiv:hep-ph/0302130.

392 [8] M. A. Lisa, S. Pratt, R. Soltz, U. Wiedemann, Femtoscopy in relativistic heavy ion collisions, Ann. Rev. Nucl. Part. Sci. 55 (2005) 357–402. arXiv:nucl-ex/0505014.

393 [9] K. Aamodt, et al., Charged-particle multiplicity density at mid-rapidity in central Pb-Pb collisions at $\sqrt{s(\text{NN})} = 2.76$ TeV arXiv:1011.3916.

394 [10] G. I. Kopylov, Like particle correlations as a tool to study the multiple production mechanism, Phys. Lett. B50 (1974) 472–474.

395 [11] G. F. Bertsch, Pion interferometry as a probe of the plasma, Nucl. Phys. A498 (1989) 173c–180c.

396 [12] S. Pratt, Pion interferometry of quark - gluon plasma, Phys. Rev. D33 (1986) 1314–1327.

397 [13] Y. Sinyukov, R. Lednicky, S. V. Akkelin, J. Pluta, B. Erazmus, Coulomb corrections for interferometry analysis of expanding hadron systems, Phys. Lett. B432 (1998) 248–257.

398 [14] J. Adams, et al., Pion interferometry in au + au collisions at $s(\text{nn})^{1/2} = 200$ -gev, Phys. Rev. C71 (2005) 044906. arXiv:nucl-ex/0411036.

399 [15] S. V. Akkelin, Y. M. Sinyukov, The hbt interferometry of expanding sources, Phys. Lett. B356 (1995) 525–530.

400 [16] Y. M. Sinyukov, Spectra and correlations in locally equilibrium hadron and quark - gluon systems, Nucl. Phys. A566 (1994) 589c–592c. doi:10.1016/0375-9474(94)90700-5.

401 [17] E. Frodermann, R. Chatterjee, U. Heinz, Evolution of pion HBT radii from RHIC to LHC – Predictions from ideal hydrodynamics, J. Phys. G34 (2007) 2249–2254. arXiv:0707.1898, doi:10.1088/0954-3899/34/11/002.

402 [18] P. Bozek, M. Chojnacki, W. Florkowski, B. Tomasik, Hydrodynamic predictions for Pb+Pb collisions at 2.76 TeV, Phys. Lett. B694 (2010) 238–241. arXiv:1007.2294, doi:10.1016/j.physletb.2010.09.065.

434 [19] M. Chojnacki, W. Florkowski, W. Broniowski, A. Kisiel, Soft heavy-ion physics from hydrodynamics with statistical hadronization: Predictions for collisions at $S^{*(1/2)}(\text{NN}) = 5.5$ -TeV, Phys. Rev. C78 (2008) 014905. arXiv:0712.0947, doi:10.1103/PhysRevC.78.014905.

435 [20] I. A. Karpenko, Y. M. Sinyukov, Energy dependence of pion interferometry scales in ultra- relativistic heavy ion collisions, Phys. Lett. B688 (2010) 50–54. arXiv:0912.3457, doi:10.1016/j.physletb.2010.03.068.

436 [21] N. Armesto, (ed.), et al., Heavy Ion Collisions at the LHC - Last Call for Predictions, J. Phys. G35 (2008) 054001. arXiv:0711.0974, doi:10.1088/0954-3899/35/5/054001.

437 [22] T. J. Humanic, Hadronic observables from Au+Au collisions at $\sqrt{s(\text{NN})} = 200$ GeV and Pb+Pb collisions at $\sqrt{s(\text{NN})} = 5.5$ TeV from a simple kinematic model, Phys. Rev. C79 (2009) 044902. arXiv:0810.0621, doi:10.1103/PhysRevC.79.044902.

438 [23] T. J. Humanic, Predictions of hadronic observables in Pb+Pb collisions at $\sqrt{s} = 2.76$ TeV from a hadronic rescattering model arXiv:1011.0378.

439 [24] M. A. Lisa, et al., Bombarding energy dependence of pion interferometry at the brookhaven ags, Phys. Rev. Lett. 84 (2000) 2798–2802.

440 [25] C. Alt, et al., Bose-Einstein correlations of pion pairs in central Pb+Pb collisions at CERN SPS energies, Phys. Rev. C77 (2008) 064908. arXiv:0709.4507, doi:10.1103/PhysRevC.77.064908.

441 [26] S. V. Afanasiev, et al., Energy dependence of pion and kaon production in central pb + pb collisions, Phys. Rev. C66 (2002) 054902. arXiv:nucl-ex/0205002.

442 [27] D. Adamová, et al., Beam energy and centrality dependence of two-pion bose-einstein correlations at sps energies, Nucl. Phys. A714 (2003) 124–144. arXiv:nucl-ex/0207005.

443 [28] B. I. Abelev, et al., Systematic Measurements of Identified Particle Spectra in pp, d^+ Au and Au+Au Collisions from STAR, Phys. Rev. C79 (2009) 034909. arXiv:0808.2041, doi:10.1103/PhysRevC.79.034909.

444 [29] K. Adcox, et al., Transverse mass dependence of two-pion correlations in au + au collisions at $s(\text{nn})^{1/2} = 130$ -gev, Phys. Rev. Lett. 88 (2002) 192302. arXiv:nucl-ex/0201008.

445 [30] K. Adcox, et al., Centrality dependence of charged particle multiplicity in Au Au collisions at $s(\text{N N})^{1/2} = 130$ -GeV, Phys. Rev. Lett. 86 (2001) 3500–3505. arXiv:nucl-ex/0012008, doi:10.1103/PhysRevLett.86.3500.

446 [31] B. B. Back, et al., Transverse momentum and rapidity dependence of HBT correlations in Au + Au collisions at $s(\text{NN})^{1/2} = 62.4$ - GeV and 200-GeV, Phys. Rev. C73 (2006) 031901. arXiv:nucl-ex/0409001, doi:10.1103/PhysRevC.73.031901.

447 [32] B. B. Back, et al., Charged-particle pseudorapidity distributions in Au+Au collisions at $s(\text{NN})^{1/2} = 62.4$ -GeV, Phys. Rev. C74 (2006) 021901. arXiv:nucl-ex/0509034, doi:10.1103/PhysRevC.74.021901.

448 [33] B. B. Back, et al., The significance of the fragmentation region in ultrarelativistic heavy ion collisions, Phys. Rev. Lett. 91 (2003) 052303. arXiv:nucl-ex/0210015, doi:10.1103/PhysRevLett.91.052303.

449 [34] C. Adler, et al., Pion interferometry of $s(\text{nn})^{1/2} = 130$ -gev au + au collisions at rhic, Phys. Rev. Lett. 87 (2001) 082301. arXiv:nucl-ex/0107008.

450 [35] A. N. Makhlin, Y. M. Sinyukov, The hydrodynamics of hadron matter under a pion interferometric microscope, Z. Phys. C39 (1988) 69.

451 [36] M. Herrmann, G. F. Bertsch, Source dimensions in ultrarelativistic heavy ion collisions, Phys. Rev. C51 (1995) 328–338. arXiv:hep-ph/9405373, doi:10.1103/PhysRevC.51.328.

452 [37] Y. M. Sinyukov, S. V. Akkelin, A. Y. Tolstykh, Interferometry

499 radii for expanding hadron resonance gas, Nucl. Phys. A610 503
500 (1996) 278c–285c. doi:10.1016/S0375-9474(96)00362-4. 504
501 [38] S. Chapman, J. R. Nix, Realistic expanding source model 505
502 for invariant one- particle multiplicity distributions and

two-particle correlations in relativistic heavy-ion collisions,
Phys. Rev. C54 (1996) 866–881. arXiv:nucl-th/9603007,
doi:10.1103/PhysRevC.54.866.